ChemComm

COMMUNICATION

View Article Online
View Journal

Cite this: DOI: 10.1039/d1cc00292a

Received 17th January 2021,
Accepted 6th February 2021

DOI: 10.1039/d1cc00292a

rsc.li/chemcomm

Multicharge β-cyclodextrin supramolecular assembly for ATP capture and drug release†

Changhui Chen, Yong Chen, Xianyin Dai, Jingjing Li, Shanshan Jia, Shuaipeng Wang and Yu Liu *

A hyaluronidase-responsive polysaccharide supramolecular assembly was constructed from an amphiphilic β-cyclodextrin bearing seven hexylimidazolium units (AMCD), adamantyl-grafted hyaluronic acid, and chlorambucil, which showed specific cancer cell targeting and controlled drug release abilities. Interestingly, ternary supramolecular assembly can disassemble in the presence of hyaluronidase, and the released AMCD can assemble with ATP to form a stable 1 : 1 complex, which enhanced the efficacy of chlorambucil on cancer chemotherapy by inhibiting ATP hydrolysis.

In clinical cancer treatment, the conventional therapeutic approach is the utilization of small molecule anticancer drugs, which usually have a number of drawbacks, such as poor water solubility, high toxicity, and a lack of specificity.[1–3] Constructing a supramolecular anti-cancer drug delivery system through supramolecular methods has become an effective method for the current treatment of cancer, which integrates therapeutic functions into self-assembling molecular vehicles and provides many practical advantages in pharmacotherapy.[4–6] More and more supramolecular drug delivery systems based on cyclodextrin, calixarene, pillararene, and cucurbituril have been constructed.[7–9] It has been proven that these supramolecular drug delivery systems can not only greatly improve the water solubility and biocompatibility of drugs, but also have specific cancer cell targeting properties. For example, Huang *et al.* fabricated a folic acid-ended diblock polymer FA-PEG-*b*-PAA to PEGylate the cationic pillar[6]arene to obtain PIC micelles, which achieved targeted drug delivery and overcome multidrug resistance in cancer therapy.[10] Wang *et al.* reported supramolecular chitosan nanogels based on Phe-grafted chitosan and CB[8], which are responsive to either endogenous or exogenous stimuli, thus allowing selective drug release in specific cancer cells or disease sites.[11] Among these macrocyclic compounds used for constructing supramolecular anti-cancer drug delivery systems, cyclodextrins (CDs) as a kind of cyclic oligosaccharide have received more and more attention and been extensively applied in the biological field owing to their low cost, negligible toxicity, good biocompatibility, and unique host–guest properties.[12–16] For example, we constructed an enzyme-responsive supramolecular polysaccharide assembly through disulfide linked adamantane–naphthalimide fluorescent camptothecin prodrug and β-CD modified hyaluronic acid, which exhibited targeted cellular imaging and controlled drug release at specific sites while providing a concurrent means for the real-time tracking of drug delivery.[17] These findings clearly indicate the great potential of supramolecular anti-cancer drug delivery system in cancer treatment.

On the other hand, adenosine triphosphate (ATP), which is called "molecular currency",[18,19] plays a crucial role in many cellular processes as one of the most important biological anions. It is the main energy source for many cell activities including cellular respiration, energy transduction, and enzyme catalysis. ATP is over-expressed in cancer cells and provides energy for various life activities of cancer cells through hydrolysis. P-Glycoprotein is a molecular pump located on the cell membrane to protect cells from invasion by foreign harmful molecules. It constantly "searches" for foreign hydrophobic molecules, just like a "security guard" that guards cells. The therapeutic drug was pumped out of the cell by P-glycoprotein against the concentration gradient, which resulted in multidrug resistance (MDR).[20–26] The whole process described above is indeed dependent on the energy provided by ATP hydrolysis. Therefore, searching for an artificial receptor with a specific selectivity for ATP has become the current research direction.

The host–guest interaction between the supramolecular macrocyclic compound and biological molecules in the aqueous phase has been extensively studied.[27,28] Due to the strong host–guest interaction, supramolecular macrocycles are ideal artificial receptors for ATP. Herein, we wish to report an enzyme-responsive supramolecular assembly based on seven hexylimidazolium modified β-cyclodextrin (AMCD) and adamantyl-grafted

College of Chemistry, State Key Laboratory of Elemento-Organic Chemistry, Nankai University, Tianjin 300071, P. R. China

† Electronic supplementary information (ESI) available: Experimental details and characterization data. See DOI: 10.1039/d1cc00292a

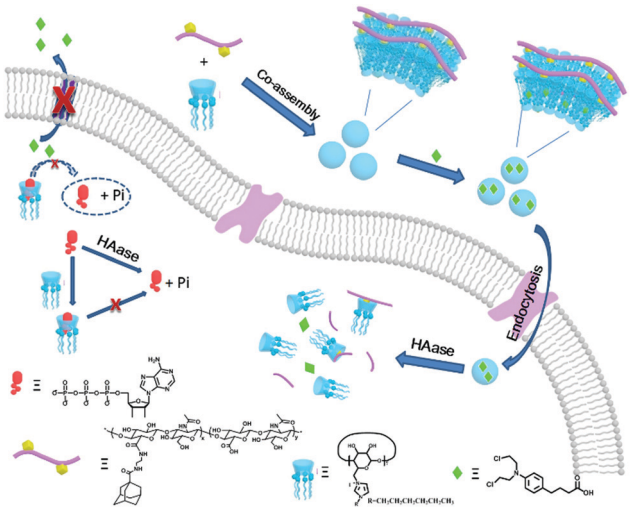

Scheme 1 Preparation of the assembly and possible mechanism to inhibit the efflux pump by forming a host–guest complex AMCD⊃ATP in the cell.

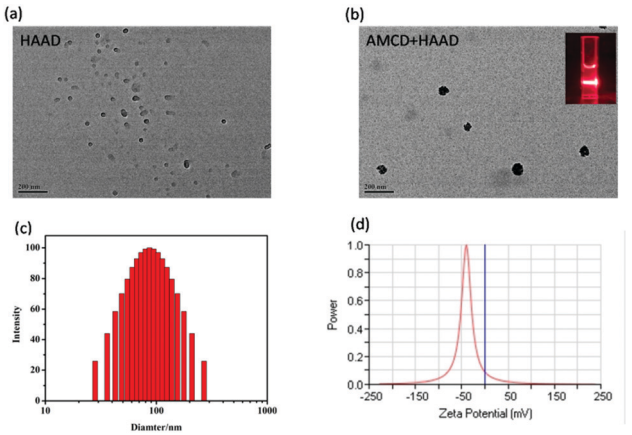

Fig. 1 The TEM images of (a) HAAD and (b) the HAAD–AMCD co-assembly; inset: Tyndall effect of the HAAD–AMCD co-assembly; (c) DLS data of the HAAD–AMCD co-assembly; (d) Zeta potential of the HAAD–AMCD co-assembly.

hyaluronic acid (HAAD). Therefore, the positive multicharged AMCD non-covalently associated with HAAD through the strong host–guest interaction between β-CD and the adamantyl group to construct a water-soluble and biocompatible supramolecular assembly HAAD–AMCD with several inherent advantages as (1) the HA skeleton enabled the targeting ability of HAAD–AMCD, (2) the assembly HAAD–AMCD has a hydrophobic layer, which can load the hydrophobic anticancer drug chlorambucil, (3) the assembly HAAD–AMCD can release anticancer drugs under the action of enzymes. AMCD has a strong binding ability to ATP due to the cyclodextrin cavity and multiple imidazole cationic groups. It can selectively complex ATP and inhibit ATP hydrolysis, thereby alleviating the multidrug resistance (MDR) of cancer cells and enhancing the efficacy of basic chemotherapy. As a result, the HAAD–AMCD assembly loaded with the anticancer drug chlorambucil (Cbl) presented a higher anticancer ability than free Cbl (Scheme 1).

Since AMCD may tend to self-aggregate in water, the critical aggregation concentration (CAC) of AMCD was measured by detecting the transmittance at various concentrations (see Fig. S3, ESI†). When the concentration of AMCD was increased, the optical transmittance of AMCD gradually decreased, which indicated the formation of aggregates in solution. An inflection point at 80 μM, assigned to the CAC, was observed on the plot of the optical transmittance of AMCD at 275 nm (T_{275}%) *versus* the concentration of AMCD. Therefore, we deduced that AMCD should exist as monomers under our experimental conditions (AMCD, 10 μM). At a concentration lower than the CAC of AMCD, HAAD–AMCD assembly could be easily constructed by simply mixing HAAD and AMCD at an adamantly group/β-CD cavity ratio of 1 : 10 in aqueous solution (Fig. S4, ESI†). A significant Tyndall effect was observed when adding HAAD (1 μM) to a solution of AMCD (10 μM). The morphological and structural features were fully investigated by transmission electron microscopy (TEM), dynamic light scattering (DLS), and Zeta potential experiments. In the TEM images, the free HAAD mainly existed as loose spherical structures with an average diameter of 35 nm (Fig. 1a), while the HAAD–AMCD assembly existed as spherical nanoparticles with an average diameter of 80 nm (Fig. 1b). The change in size of nanoparticles indicated that HAAD and AMCD are assembled. As is shown in Fig. 1c, the diameter of HAAD–AMCD was approximately 82 nm from DLS, which was very close to the results of TEM. Since the carboxyl groups on the HA backbone are ionized, the measured zeta potential of the assembly was approximately −40.19 mV (Fig. 1d). This negatively charged surface will promote the stability and biocompatibility of the assembly in the biological environment and extend its circulation time in the body.[29–31]

Then, we investigated the HAase response of the HAAD–AMCD assembly. The samples with and without HAase stayed at 37 °C for six hours. As shown in Fig. S5a and b (ESI†), the transmittance of HAAD–AMCD increased significantly after the addition of HAase, indicating the disappearance of the large aggregates. Besides, TEM images indicated that there were no spherical aggregates after adding HAase to HAAD–AMCD for six hours. Moreover, no appreciable Tyndall effect was observed after the addition of HAase for about six hours (Fig. S5c, ESI†).

The capability of the HAAD–AMCD assembly to load drugs was examined by using chlorambucil (Cbl), an efficient anticancer drug, as a model substrate. A series of Cbl with different concentrations from 5 mg L^{-1} to 50 mg L^{-1} were measured to obtain the standard curve of Cbl (Fig. S6, ESI†). A new band at 257 nm, which was assigned to the characteristic absorption of Cbl, appeared in the UV-vis spectrum of Cbl@HAAD–AMCD. The absorption of HAAD–AMCD as the reference was deducted from the UV-vis spectrum of Cbl@HAAD–AMCD (Fig. S7, ESI†), and then the net concentration of Cbl could be calculated according to the standard curve of CbI at 257 nm. Therefore, the Cbl loading efficiency and the encapsulation efficiency were calculated as 9.4% and 64.1%, respectively. Moreover, TEM images showed that the HAAD–AMCD assembly retained the original structural features after loading Cbl. Also, the Cbl release rate of the Cbl@HAAD–AMCD assembly was examined.

The Cbl release experiment was carried out by adding HAase to the solution of Cbl@HAAD–AMCD co-assembly and the system was kept at 37 °C for 12 h. Then the solution was dialyzed to measure the released Cbl. The result showed that nearly half of the Cbl was released in the first two hours, and *ca.* 91.8% of the Cbl was released in twelve hours (Fig. S8, ESI†).

The host–guest interactions between AMCD and ATP were studied by ^{1}H NMR spectroscopy (Fig. S9, ESI†). Compared with the free guest (ATP), chemical shift changes were observed for the protons in the presence of AMCD. The active hydrogen on imidazole in AMCD had no signal, but in the AMCD ⊃ ATP complex, we found the active hydrogen signal on AMCD imidazole. This is due to the charge interaction between the imidazole cation of AMCD and the phosphate group on ATP, which stabilized the active hydrogen of the imidazole, thereby generating a detectable signal. Furthermore, ROESY correlation signals were observed between protons H_a, and H_b on the adenosine unit of ATP and protons H_1, H_2, H_3, and H_4 on the cyclodextrin, indicating that ATP penetrated the cavity of AMCD to form a [2]pseudorotaxane-type inclusion complex (Fig. S10, ESI†). Since AMCD itself could aggregate at a very low concentration, we synthesized per-6-deoxy-6-(1-methylimidazol-3-*ium*-3-yl)-β-CD (AMCD-1β) as a model molecule according to the reported method.[32] Isothermal titration calorimetry (ITC) experiments were further performed to quantitatively determine the association constant (K_S) of AMCD-1β with ATP (Fig. 2) as 1.32×10^5 M^{-1}. The enthalpy and entropy changes were both positive ($\Delta H > 0$; $T\Delta S > 0$) and $|\Delta H| < |T\Delta S|$, indicating that the complexation was driven by entropy changes.

Next, the stability of the AMCD ⊃ ATP complex was tested. The ^{31}P NMR spectra indicated that the hydrolysis rate of ATP slowed down efficiently by forming a stable host–guest inclusion complex AMCD ⊃ ATP in the presence of CIAP (10 U mL^{-1})

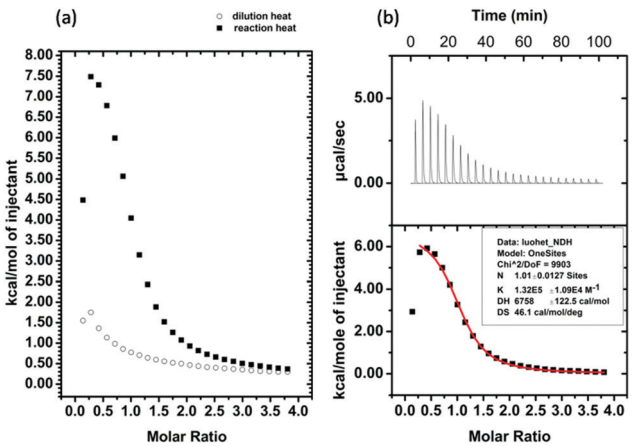

Fig. 2 (a) Heat effects of the dilution and of the complexation reaction of ATP with AMCD for each injection during the titration microcalorimetric experiment. (b) Microcalorimetric titration of ATP with AMCD-1β in PBS (pH = 7.4) at 298.15 K. (Top) Raw ITC data for 25 sequential injections (10 μL per injection) of an ATP solution (2.00 mM) into an AMCD-1β solution (0.1 mM). (Bottom) Net reaction heat obtained from the integration of the calorimetric traces.

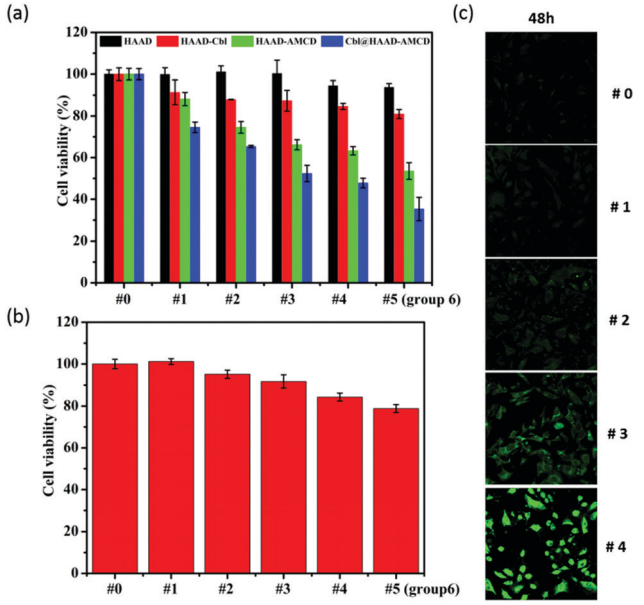

Fig. 3 (a) Cytotoxicity of HAAD, HAAD-Cbl, HAAD–AMCD, and Cbl@HAAD–AMCDHAAD–AMCD towards A549 cancer cells. # 0: control experiment, # 1: [HAAD] = 2.18 mg L^{-1}, [AMCD] = 29.7 mg L^{-1}, [Cbl] = 3.21 mg L^{-1}, the concentration of all components of # 2, # 3, # 4, # 5 are 2, 4, 6, 8 times that of # 1. (b) Cytotoxicity of Cbl@HAAD–AMCD towards 293T cells. # 0: control experiment, #1 [HAAD] = 2.18 mg L^{-1}, [AMCD] = 29.7 mg L^{-1}, [Cbl] = 3.21 mg L^{-1}, the concentration of all components of # 2, # 3, # 4, # 5 are 2, 4, 6, 8 times that of # 1. (c) Confocal laser scanning microscopy images of the A549 cells stained with calcein-AM incubated without/with HAAD, and HAAD–AMCD assembly at different concentrations; # 0: control experiment, # 1: [HAAD] = 21.8 mg L^{-1}, # 2: [HAAD] = 2.18 mg L^{-1}, [AMCD] = 29.7 mg L^{-1}, the concentration of all components of # 3, # 4 are 5, 10 times that of # 2.

(Fig. S11 and S12, ESI†). The reason may be that ATP was located in the hydrophobic cavity of AMCD, preventing ATP from being hydrolyzed. Over-expression of the drug efflux pump is one of the major causes of MDR, which transports anticancer drugs out of the cells and results in drug resistance by utilizing the energy from ATP hydrolysis. P-Glycoprotein was upregulated in the plasma membrane of all MDR cancer cells, which was known as the ATP-dependent drug efflux pump. If the hydrolysis of ATP was inhibited, the energy supply of cancer cells will decrease, resulting in the blocking of the efflux pump. On the other hand, anticancer drugs will maintain an effective concentration for a long time because the drug efflux pump did not work. Therefore, the AMCD in this system could significantly improve the efficacy of cancer chemotherapy.

Subsequently, cytotoxicity experiments towards A549 cancer cells were performed to evaluate the anticancer activity of Cbl@HAAD–AMCD *in vitro* by CCK8 assay. As shown in Fig. 3a, all six groups exhibited a dose-dependent killing effect towards cancer cells after incubation for 48 h. HAAD exhibited no obvious toxicity to A549 cells in # 5 ([HAAD] = 17.44 mg L^{-1}). However, the cell viability of HAAD-Cbl was also relatively high, reaching 80.94% in # 5 ([HAAD] = 17.44 mg L^{-1}, [Cbl] = 25.68 mg L^{-1}). We speculated that chlorambucil (Cbl) was an extremely hydrophobic anticancer drug, which was

difficult to be effectively worked in the absence of a carrier, although its anti-cancer effect was very good. To our delight, HAAD–AMCD showed a great cancer cell inhibitory effect, and the cell viability was only close to 50% in #5 ([HAAD] = 17.44 mg L^{-1}, [AMCD] = 237.6 mg L^{-1}). We suggested that the assembly targeted the cancer cells and released AMCD under the action of hyaluronidase. Then, AMCD selectively complexed with ATP and formed a stable 1 : 1 AMCD ⊃ ATP assembly to prevent ATP hydrolysis and cut off the energy supply of cancer cells, which inhibited the normal activities of cancer cells. Cbl@HAAD–AMCD assembly showed the best effect with the cell viability of 35% in #5 ([HAAD] = 17.44 mg L^{-1}, [AMCD] = 237.6 mg L^{-1}, [Cbl] = 25.68 mg L^{-1}). This further verified that the hydrophobic anticancer drug was loaded on the assembly, which thus enhances the effect of basic chemotherapy in the presence of AMCD. Besides, low cytotoxicity could be observed on the human embryonic kidney normal cell line 293T cells (Fig. 3b). Then, confocal laser scanning microscopy experiments were designed to examine the effect of ATP capture on P-glycoprotein. Calcein-AM can diffuse across the cell membranes by its hydrophobicity, which was utilized as a probe to test the activity of the efflux pumps in cell membranes by monitoring the fluorescence intensity.[33] As shown in Fig. 3c, the fluorescence intensity of the A549 cells in the control experiment became weaker after culturing the cells for 48 h, indicating that hydrolyzed calcein was pumped out due to the ATP hydrolysis. A similar phenomenon was observed for cells under the same incubation conditions in the presence of HAAD. While the fluorescence intensity of the cells changes much slower in the presence of AMCD owing to the inhibition of ATP hydrolysis forming AMCD ⊃ ATP. Of course, the inhibition of ATP hydrolysis will induce other biological effects on the cell beyond the suppression of P-glycoprotein. Hence, it is certain that this effect is worthy of further study.

In conclusion, the water-soluble seven hexylimidazolium modified amphiphilic cyclodextrin selectively combined with ATP to form a stable 1 : 1 inclusion complex AMCD ⊃ ATP, which was mainly driven by entropy changes. As a result, due to the presence of the hydrophobic cavity of AMCD, the hydrolysis of ATP was effectively inhibited. The hydrophobic anticancer drug Cbl was loaded in an assembly of adamantyl-grafted hyaluronic acid and an amphiphilic β-cyclodextrin bearing seven hexylimidazolium units. The assembly could specifically target cancer cells and respond to hyaluronidase thus releasing the anticancer drug CbI. Moreover, the AMCD and ATP formed a host–guest inclusion complex, which cut off the energy supply of cancer cells and thus could effectively alleviate the multidrug resistance of cancer cells. CCK8 analysis showed that in the presence of AMCD, the efficacy of the anti-cancer drug Cbl has been effectively improved. The results of this study indicated that the amphiphilic cyclodextrin can overcome the multidrug resistance in cancer treatment to some extent and is expected to become a synergistic carrier for enhanced chemotherapy, providing an assembled strategy based on multicharged cyclodextrin for cancer treatment.

We thank NNSFC (No. 21861132001, 21971127, 21772099) for financial support.

Conflicts of interest

There are no conflicts to declare.

Notes and references

1 P. Huang, D. Wang, Y. Su, W. Huang, Y. Zhou, D. Cui, X. Zhu and D. Yan, *J. Am. Chem. Soc.*, 2014, **136**, 11748.
2 J. Zhou, G. Yu and F. Huang, *Chem. Soc. Rev.*, 2017, **46**, 7021.
3 Y. Chen, Z. Huang, H. Zhao, J.-F. Xu, Z. Sun and X. Zhang, *ACS Appl. Mater. Interfaces*, 2017, **9**, 8602.
4 L.-L. Tan, H. Li, Y. Zhou, Y. Zhang, X. Feng, B. Wang and Y.-W. Yang, *Small*, 2015, **11**, 3806.
5 P. Xing and Y. Zhao, *Small Methods*, 2018, **2**, 1700364.
6 G. Sun, Z. He, M. Hao, M. Zuo, Z. Xu, X.-Y. Hu, J.-J. Zhu and L. Wang, *J. Mater. Chem. B*, 2019, **7**, 3944.
7 Z. Liu, X. Dai, Y. Sun and Y. Liu, *Aggregate*, 2020, **1**, 31.
8 H.-B. Cheng, Y.-M. Zhang, Y. Liu and J. Yoon, *Chemistry*, 2019, **5**, 553.
9 M. Cen, Y. Ding, J. Wang, X. Yuan, B. Lu, Y. Wang and Y. Yao, *ACS Macro Lett.*, 2020, **9**, 1558.
10 G. Yu, J. Zhou, J. Shen, G. Tang and F. Huang, *Chem. Sci.*, 2016, **7**, 4073.
11 Y.-F. Ding, J. Wei, S. Li, Y.-T. Pan and R. Wang, *ACS Appl. Mater. Interfaces*, 2019, **11**, 28665.
12 Y.-M. Zhang, Q.-Y. Xu and Y. Liu, *Sci. China: Chem.*, 2019, **62**, 549.
13 Y. M. Zhang, Y. H. Liu and Y. Liu, *Adv. Mater.*, 2020, **32**, 1806158.
14 G. Yu, X. Zhao, J. Zhou, Z. Mao, X. Huang, Z. Wang, B. Hua, Y. Liu, F. Zhang, Z. He, F. Huang and X. Chen, *J. Am. Chem. Soc.*, 2018, **140**, 8005.
15 F.-Q. Li, Q.-L. Yu, Y.-H. Liu, H.-J. Yu, Y. Chen and Y. Liu, *Chem. Commun.*, 2020, **56**, 3907.
16 S. Qie, Y. Hao, Z. Liu, J. Wang and J. Xi, *Acta Chim. Sin.*, 2020, **78**, 232.
17 Y.-H. Zhang, Y.-M. Zhang, X. Sheng, J. Wang and Y. Liu, *Chem. Commun.*, 2020, **56**, 1042.
18 C. Devadoss, P. Bharathi and J. S. Moore, *J. Am. Chem. Soc.*, 1996, **118**, 9635.
19 G. M. Stewart and M. A. Fox, *J. Am. Chem. Soc.*, 1996, **118**, 4354.
20 C. F. Higgins and K. J. Linton, *Nat. Struct. Mol. Biol.*, 2004, **11**, 918.
21 M. F. Fromm, *Trends Pharmacol. Sci.*, 2004, **25**, 423.
22 W. Jin, Q. Wang, M. Wu, Y. Li, G. Tang, Y. Ping and P. K. Chu, *Biomaterials*, 2017, **129**, 83.
23 M. M. Gottesman, T. Fojo and S. E. Bates, *Nat. Rev. Cancer*, 2002, **2**, 48.
24 G. Taubes, *Science*, 2008, **321**, 356.
25 N. Z. Kuhn and L. Nagahara, *Mol. Pharmaceutics*, 2011, **8**, 1994.
26 I. Brigger, C. Dubernet and P. Couvreur, *Adv. Drug Delivery Rev.*, 2012, **64**, 24.
27 Y.-M. Zhang, Y.-H. Liu and Y. Liu, *Adv. Mater.*, 2020, **32**, 1806158.
28 Y. Chen, F. Huang, Z.-T. Li and Y. Liu, *Sci. China: Chem.*, 2018, **61**, 979.
29 H. S. S. Qhattal, T. Hye, A. Alali and X. Liu, *ACS Nano*, 2014, **8**, 5423.
30 Y. Yang, Y.-M. Zhang, Y. Chen, J.-T. Chen and Y. Liu, *J. Med. Chem.*, 2013, **56**, 9725.
31 Q. Zhao, Y. Chen, M. Sun, X.-J. Wu and Y. Liu, *RSC Adv.*, 2016, **6**, 50673.
32 D. Zhao, Y. Chen and Y. Liu, *Chin. Chem. Lett.*, 2015, **26**, 829.
33 Z. Mao, R. Cartier, A. Hohl, M. Farinacci, A. Dorhoi, T.-L. Nguyen, P. Mulvaney, J. Ralston, S. H. E. Kaufmann, H. Mohwald and D. Wang, *Nano Lett.*, 2011, **11**, 2153.

